JOURNAL OF MATERIALS SCIENCE **36** (2001) 5045–5056

A new empirical formula for the bainite upper temperature limit of steel

ZHENBO ZHAO, CHENG LIU
Mechanical, Materials and Automotive Engineering, University of Windsor, Windsor, Ontario, Canada, N9B 3P4

YUNXU LIU
Department of Materials Engineering, Jilin Institute of Technology, Changchun, Jilin, 130012, People's Republic of China

D. O. NORTHWOOD
Faculty of Engineering & Applied Science, Ryerson Polytechnic University, Toronto, Ontario, Canada, M5B 2K3

The definition of the practical upper temperature limit of the bainite reaction in steels is discussed. Because the theoretical upper temperature limit of bainite reaction, B_0, can neither be obtained directly from experimental measurements, nor from calculations, then, different models related to the practical upper temperature limit of bainite reaction, B_S, are reviewed and analyzed first in order to define the B_0 temperature. A new physical significance of the B_S and B_0 temperatures in steels is proposed and analyzed. It is found that the B_0 temperature of the bainite reaction in steels can be defined by the point of intersection between the thermodynamic equilibrium curve for the austenite→ferrite transformation by coherent growth (curve $Z_{\gamma\rightarrow\vec{\alpha}}$) and the extrapolated thermodynamic equilibrium curve for the austenite→cementite transformation (curve ES in the Fe-C phase diagram). The B_S temperature for the bainite reaction is about 50–55 °C lower than the B_0 temperature in steels. Using this method, the B_0 and B_S temperatures for plain carbon steels were found to be 680 °C and 630 °C, respectively. The bainite reaction can only be observed below 500 °C because it is obscured by the pearlite reaction which occurs prior to the bainite reaction in plain carbon steels. A new formula, B_S(°C) =,630-45Mn-40V-35Si-30Cr -25Mo-20Ni-15W, is proposed to predict the B_S temperature of steel. The effect of steel composition on the B_S temperature is discussed. It is shown that B_S is mainly affected by alloying elements other than carbon, which had been found in previous investigations. The new formula gives a better agreement with experimental results than for 3 other empirical formulae when data from 82 low alloy steels from were examined. For more than 70% of these low alloy steels, the B_S temperatures can be predicted by this new formula within ±25°C. It is believed that the new equation will have more extensive applicability than existing equations since it is based on data for a wide range of steel compositions (7 alloying elements).

1. Introduction

It is well known that the practical and theoretical upper temperature limits (the highest equilibrium temperatures) of the pearlite reaction are the A_{r1} and A_{c1} temperatures. For the martensite reaction, the practical and theoretical upper temperature limits are the M_S and M_0 temperatures, respectively. Both of these, i.e. pearlite and martensite, have been investigated extensively. However, little, or no work has been reported on the practical and theoretical upper temperature limits, B_S and B_0, for the bainite reaction. A knowledge of B_S and B_0 temperature is very useful in defining the thermodynamic conditions of the bainite reaction and in establishing the intrinsic relationship among the three decomposition products of austenite.

In plain carbon steels, because the pearlite transformation is diffusion-controlled (carbon and iron atoms), the A_{c1} temperature can be determined by the intersection of the austenite→ferrite thermodynamic equilibrium curve ($Z_{\gamma\rightarrow\alpha}$) (curve GS) and the austenite→cementite thermodynamic equilibrium curve ($Z_{\gamma\rightarrow c}$) (curve ES). It is independent of carbon content. The martensite transformation occurs via coherent shear at M_0. Thus, the M_0 temperature is determined by the thermodynamic equilibrium curve $Z_{\gamma\rightarrow\vec{\alpha}(c)}$ (curve T_0). T_0 is defined as the thermodynamic equilibrium curve ($Z_{\gamma\rightarrow\alpha(c)}$) for the austensite→ α-Fe(c) (ferrite which is super-saturated by carbon) transformation. However, because a higher free energy is needed for the coherent growth of ferrite, the curve

$Z_{\gamma\to\alpha(c)}$ should be above the curve $Z_{\gamma\to\vec{\alpha}(c)}$ (the thermodynamic equilibrium curve for the austenite→ferrite transformation by coherent growth). Only $Z_{\gamma\to\vec{\alpha}(c)}$ agrees well with the values of M_0 calculated using the formula $\frac{1}{2}(M_S + A_S)$ or $\frac{1}{2}(M_d + A_d)$ (Here A_S and A_d represent the austenite start point and the deformed austenite start point in transformation hysteresis for thermoelastic martensite.) Therefore, the curve T_0 should be curve $Z_{\gamma\to\vec{\alpha}(c)}$, rather than the curve $Z_{\gamma\to\alpha(c)}$ in a displacive transformation.). The M_0 temperature decreases with increasing carbon content. In spite of this, there are still uncertainties with respect to the B_0 and B_S temperatures of steel, such as their physical significance, the effect of alloying elements on them and their exact value in plain carbon steels.

2. Previous theories and models for the B_S temperature in steels

The B_0 temperature can neither be directly obtained from experimental measurements, nor by calculation. In order to obtain the B_0 temperature, the only method is to first define the B_S temperature, then derive the B_0 temperature from the B_S temperature. Therefore, it is necessary to first examine the Bs temperature.

Thus far, there appears to be no general agreement regarding the physical significance of the B_S temperature in steels. There have been only three purely empirical formulae developed to calculate the effect of alloying elements on the B_S temperature [1–3]. However, no physical significance can be correctly described when all alloying elements become zero and only carbon left (i.e. for plain carbon steel) from these three formulae. Also, due to either a limited number of alloying elements involved, or the poor accuracy of the resulting predictions, the application range for these 3 equations is relatively narrow. This may be related to the bainite reaction itself with uncertainties with respect to reaction mechanisms and thermodynamic models [4, 5].

In order to help define the B_S temperature, several different theories and models had been proposed. Davenport and Bain [6] originally suggested that bainite forms as supersaturated ferrite, with cementite then precipitating in the ferrite. In support of this theory, Zener [7] showed that the upper temperature limit for bainite formation was approximately equal to the temperature corresponding to a zero free-energy change for the austenite→super-saturated ferrite transformation. He postulated that kinetic bainite 'inherits' the carbon, as well as the alloy content, of the parent austenite. The kinetic-B_S temperature* is thus identical to the T_0 temperature, which is the temperature at which austenite and ferrite of the same composition are in a stress-free equilibrium. This theory explains, at least qualitatively, most of the kinetic bainite phenomena [5]. A

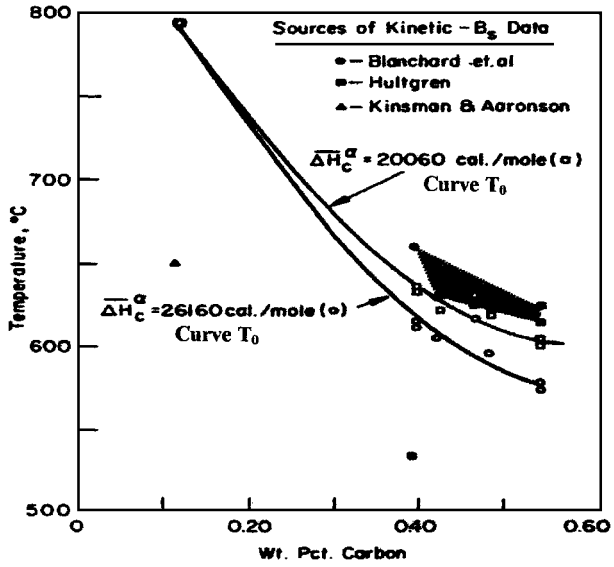

Figure 1 Effect of carbon content upon the kinetic-B_S and T_0 temperatures [5, 8–10].

straightforward theoretical test of this theory was made by Aaronson [5] who compared the calculated T_0 temperatures with the experimentally determined kinetic-B_S temperatures: see Fig. 1. The data on the kinetic-B_S temperatures which were obtained from published TTT diagrams [8–10] and the T_0 temperatures calculated for these steels are plotted in Fig. 1 as function of carbon content.

All but two of the kinetic-B_S data points lie within the rather narrow shaded region, and are in reasonable agreement with the higher of the two T_0 curves. The steels in this group all contained between 0.39 and 0.54 wt%C, and from 0.23 to 0.82 wt%Mo. The two exceptions, however, lie far below the T_0 curves. Aaronson [5] postulated that the agreement between the kinetic-B_S and the T_0 temperatures might be coincidental, and that the kinetic-B_S temperature had no fundamental significance.

Fisher [11]'s original model for the bainite reaction assumed that the transformation was martensitic, but was lacking the strain energy that accompanies the formation of martensite. He was therefore able to explain why bainite is observed to form at temperatures above M_S but below T_0. He considered that the bainite reaction first involves the transformation from austenite to supersaturated ferrite, which then decomposes into the 'mixture', bainite, which includes both ferrite and the carbide. Therefore, he suggested that the B_S temperature should be below the austenite→ferrite thermodynamic equilibrium curve (curve T_0). In addition, due to the effects of diffusion of carbon in austenite on transformation during precipitation of bainite, the B_S temperature is also above the M_S temperature. The B_S and M_S temperatures are similar and both gradually decrease with increasing carbon content in steels. Lyman's [12] experimental data for the B_S temperature for steels with 3 wt%Cr and carbon contents ranging from 0.08 to 1.28 wt%C were used by Fisher to support his model: see Fig. 2.

Gyljaev [13] suggested that the bainite reaction begins with the formation of ferrite nuclei. On the growth

* In terms of a kinetic definition[5], it is recognised that the bainite reaction has its own C-curve for the initiation of the transformation on a TTT diagram. The upper temperature of the bainite C-curve, previously denoted as the "kinetic-bainite start" or "kinetic-Bs" temperature, represents the highest temperature at which bainite can form, and usually lies 100–300 °C below the eutectoid temperature range. The proportion of the austenite transformed to bainite decreases with increasing temperature, and becomes zero at the kinetic-B_S temperature.

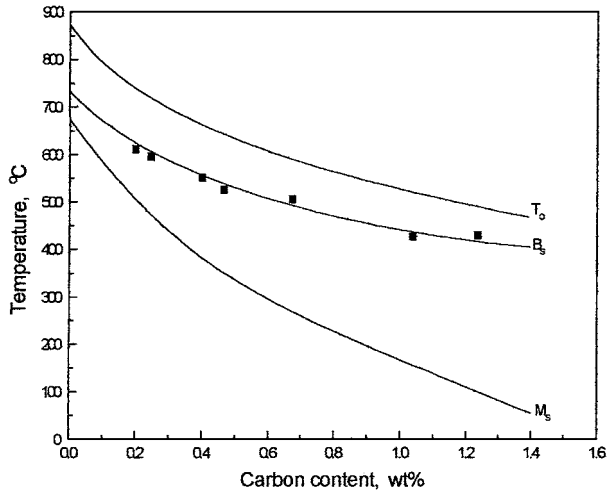

Figure 2 B_S, T_0 and M_S as a function of carbon content [11]. (The solid square points represent the experimental results of Lyman [12] for the B_S temperature).

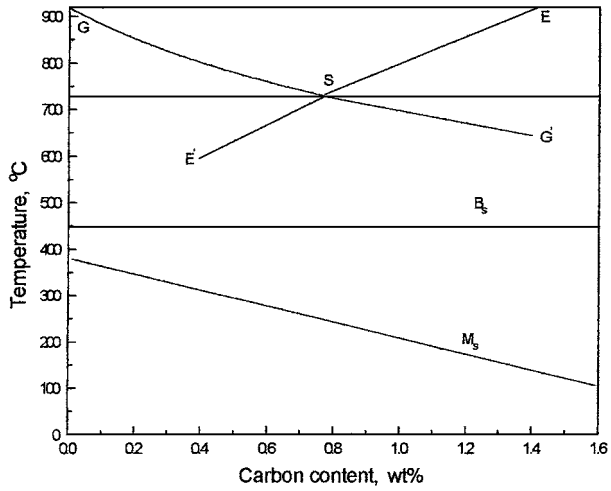

Figure 3 Schematic diagram of Gyljaev's model [13].

of the ferrite nuclei, plastic glide takes place at and around the austenite due to the effects of stress. Precipitation of the carbide is then initiated in the deformed austenite. The growth of the ferrite can continue after the internal stress relief which accompanies plastic glide. Therefore, the bainite reaction occurs below the recrystalization temperature, but is independent of the carbon content in the steel (unfortunately, he did provide any explanation as to why the B_S temperature is independent of the carbon content). The B_S temperature from this model is 450 °C for a plain carbon steel: see Fig. 3 for a schematic diagram of Gyljaev's model.

The model of Blanter [14] also had the bainite reaction starting from the ferrite nuclei formed in the austenite. However, he proposed that after the formation of ferrite nuclei, carbon both within the austenite and that 'located' around the ferrite will diffuse away, or transform into the carbide. This then promotes the growth of ferrite with diffusionless and coherent characteristics. The newly formed ferrite is supersaturated in carbon and will decompose into a mixture of ferrite and carbide, i.e. Bainite, with near equilibrium concentration (determined by the Fe-C phase diagram). Blanter concluded that the upper temperature limit of the bainite reaction should be the temperature at which the low

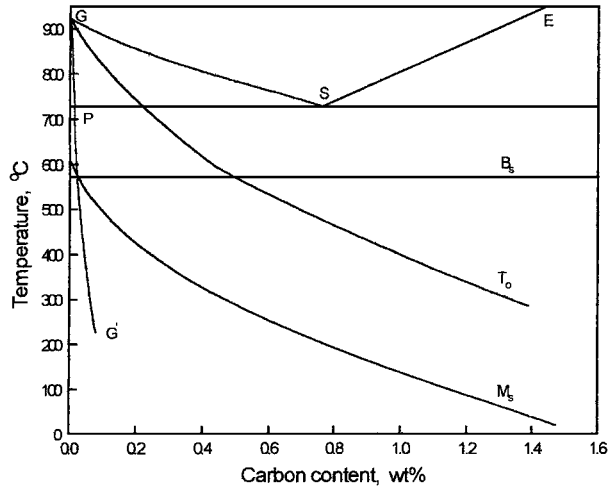

Figure 4 Schematic diagram of Blanter's model [14].

carbon austenite is transformed into ferrite by coherent growth. This corresponds to a temperature which is just below the intersection of the M_S curve and the extrapolated GP curve (the solidus line from austenite to ferrite in Fe-C phase diagram). The B_S temperature is again independent of carbon content as shown in Fig. 4.

Kriesement and Wever [15], however, suggested that carbon migration would occur first, followed by the nucleation of ferrite by coherent growth (for low carbon steels) or carbide (for high carbon steels). Growth of the nuclei is due to carbon migration. They pointed out that the appearance of bainite continuously changes from upper to lower bainite, and postulated that the growth of bainite involves the repeated and alternate nucleation and growth of lamellae of cementite and ferrite from the austenite. Thus, they suggested that the upper temperature limit for the bainite reaction can be determined from the intersection temperature of the thermodynamic equilibrium curve for the austenite→ferrite transformation (curve T_0) and the extrapolated thermodynamic equilibrium curve for the austenite→cementite transformation (curve ES in the Fe-C phase diagram): see Fig. 5 for a schematic diagram. A similar trend was obtained after they put the data (the alloy element content of all experimental steels was below 1%) of Hulfgren [9] into Fig. 5.

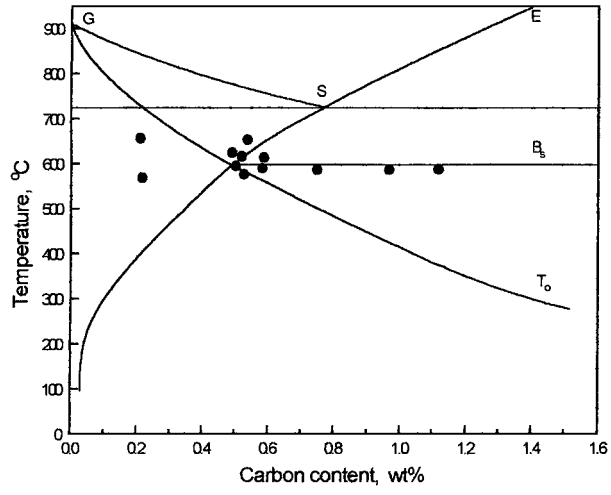

Figure 5 Schematic diagram of Kriesement and Wever's model [15]. (The solid points represent the experimental results of Hulfgren [9].)

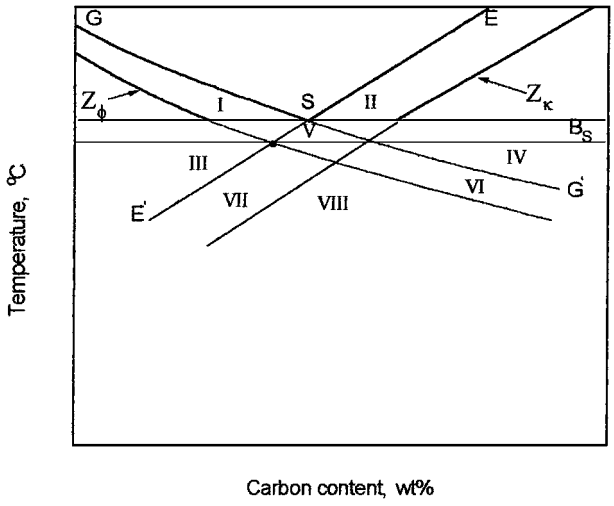

Figure 6 Schematic diagram of Leont'ev's model [16].

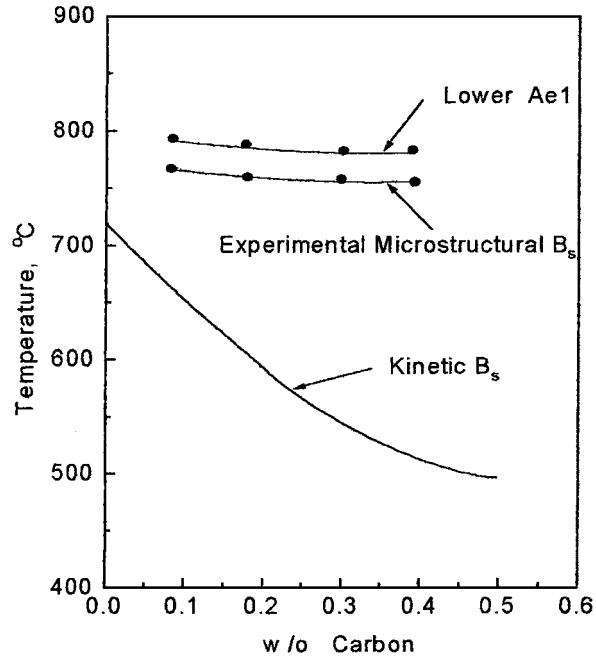

Figure 7 Effect of carbon content upon the lower Ae1 temperature, the experimentally observed microstructural-B_S, and the TTT diagram or kinetic-B_S (as reported by Lyman and Troiano [12]) in 3%Cr steels [5].

The Fe-C phase "state" diagram proposed by Leont'ev [16] showed the thermodynamic equilibrium curves for austenite → ferrite (curve GS), austenite → cementite (curve ES), austenite → ferrite by displacive growth (curve Z_Φ) and austenite → cementite by displacive growth (curve Z_k) (see Fig. 6). Leont'ev suggested that bainite could be precipitated in areas VII and VIII. He suggested that the upper temperature limit for the bainite reaction is the horizontal line corresponding to the intersection point between the curve $Z_{\vec{\Phi}}$ and the extrapolation of curve ES.

Aaronson [5] regarded bainite simply as a non-lamellar two-phase aggregate of ferrite and carbides in which the phases form consecutively (as distinct from pearlite where they form cooperatively). Aaronson suggested that if one restricted the use of the term bainite to structures in which the ferritic component has a plate or needle morphology, the microstructural B_S temperature in high-purity Fe-C alloys varies with carbon content from around 520 °C to 580 °C (for steels containing 0.3–1.65 wt%C).

When microstructurally-defined bainite is freed of this morphological restriction, however, the microstructural B_S temperature becomes almost identical to the eutectoid temperature for carbides precipitated both from austenite at austenite/ferrite boundaries and from ferrite. Experimental results for a 3%Cr steel [5] support this conclusion by providing evidence for carbide precipitation from impinged aggregates of proeutectoid ferrite allotriomorphs at a temperature only 20 °C below the lower eutectoid temperature. However, as can be seen from Fig. 7 [5] this result was only seen for a relatively narrow range of carbon contents (0.08 wt% to 0.4 wt%). A schematic TTT curve proposed by Aaronson [5] for the initiation of the bainite reaction is shown in Fig. 8. The "C" curve for bainite reaction has been drawn asymptotic to a line just below the eutectoid temperature to indicate the location of the revised microstructural-B_S, and is broken at high temperatures to make clear that whether or not bainite actually appears at these temperatures, depends greatly on the proeutectoid ferrite and pearlite microstructures initially generated.

In spite of all these uncertainties regarding the bainite reaction, some agreement has been achieved. It has been found [9, 15, 17] that the practical upper temperature limit for the bainite reaction, B_S, has no obvious relationship to the carbon content of the steel.

Aaronson's analysis [5] contradicted Zener's model [7] as described earlier. Aaronson [5] postulated that the agreement between the kinetic-B_S and the T_0 temperatures suggested by Zener might be coincidental, and that the kinetic-B_S temperature had no fundamental significance. Also, the experimental results of Hultgren[9] used by Kriesement and Wever [15] corrected the deviation of Lyman's report [9] which was used to support Fisher's model. Therefore, the conclusion of Fisher about B_S temperature also should be excluded. Given that the practical upper temperature for the bainite reaction in many steels lies either above 450 °C [18–20] or below the eutectoid temperature (A_{e1}) [20], it is reasonable to conclude that the models of Gyljaev [13] and Aaronson [5] for the B_S temperature are probably only valid over a relatively narrow range of carbon contents. The model of Blanter [14] for the B_S temperature is able to explain the temperature conditions and characteristics of ferrite formation, but does not consider the temperature conditions and characteristics for carbide formation. The practical upper temperature limit of the bainite reaction (namely the intersection point of curve T_0 and the extrapolated curve of ES) as suggested by Kriesement and Wever [15] can be considered the theoretical upper temperature limit for the bainite reaction, but it is not, of course, the B_S temperature. Although some data of Hultgren were in agreement with the model of Kriesement and Wever [15], there are a number of data points located above the T_0 curve (see Fig. 5.). This indicates that the model of Kriesement and Wever for the B_S temperature requires further refinement. The model of Leont'ev [16] only suggested

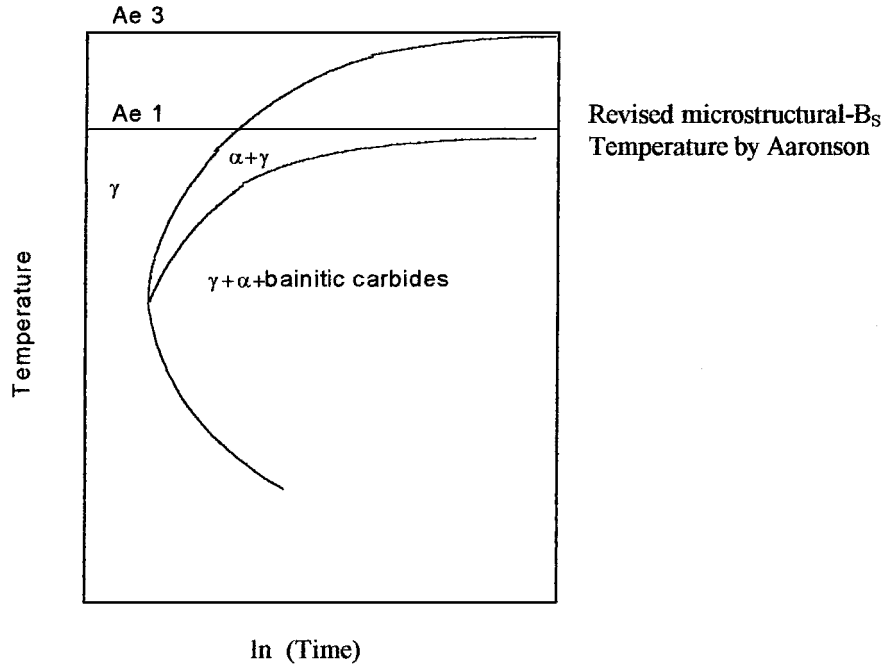

Figure 8 Schematic TTT diagram for the initiation of the proeutectoid ferrite reaction (solid curve) and of the associated precipitation of bainitic carbides (broken curve) [5].

a conceptual definition for the upper temperature limit of the bainite reaction, but did not provide any practical temperature data as a reference point. Given these uncertainties, a new model for the B_S and B_0 temperatures is proposed in Section 3.

3. The physical significance of the B_S and B_0 temperatures in steels

In microstructural terms [21], bainite can be defined as acicular Widmanstatten ferrite which is precipitated from austenite and contains a (normally) non-lamellar dispersion of carbides (or cementite). The coherent growth of the Widmanstatten ferrite retains the orientation relationships with the parent phase. Also, the Widmanstatten ferrite and the carbides of the upper bainite, grow simultaneously with different microstructures from tempered martensite under the same temperature conditions.

Aaronson [5] reported that whether the non-lamellar (bainite) or the lamellar (pearlite) form of the eutectoid reaction occurs in a given steel at a given temperature below that of the eutectoid, is a complex question of competitive reaction kinetics, rather than of thermodynamics. He recommended that the generalized microstructural definition should be adopted as the definition for bainite, and this has been adopted in this paper.

Since, as discussed previously, the B_0 temperature can not be obtained directly, the B_S temperature for steels will be analyzed and discussed first, and then the B_0 temperature will be derived from the B_S temperature.

In order to differentiate the B_S temperature proposed in this paper from the "kinetic-B_S," B_S is designated as the bainite practical upper temperature limit (it is a horizontal line at the highest temperature that bainite can form.), rather than the bainite start temperature (this is a C shaped curve that shows when bainite starts to form.). It is our opinion that the B_S point should be defined according to both thermodynamic and kinetic criteria, as the bainite practical upper temperature limit, i.e. in the same manner as the A_1, A_3, and M_S temperatures are defined. It should not be affected by cooling velocity, since it is generally accepted that the ferrite component of bainite inherits the carbon content of the parent austenite no matter how slow the cooling velocity [21, 22]. Thus, regardless of whether it is an isothermal transformation (IT) diagram or a continuous cooling transformation (CCT) diagram, the B_S temperature should be the same. For those diagrams in which there is no appreciable overlap of the bainite and pearlite transformation ranges, the B_S temperature should be a horizontal line that is infinitely approached by the upper half of the asymptotes of the lower C curves [23].

In terms of the above analysis, it is reasonable to propose that the theoretical upper temperature limit, B_0, of the bainite reaction should be determined by the intersection point between the thermodynamic equilibrium curve for the austenite → ferrite trasnformation by coherent growth ($Z_{\gamma\rightarrow\vec{\alpha}}$) and the extrapolated thermodynamic equilibrium curve for the austenite → cementite ($Z_{\gamma\rightarrow C}$) transformation (curve ES). However, the thermodynamic equilibrium curve for the austenite → ferrite transformation by coherent growth ($Z_{\gamma\rightarrow\vec{\alpha}}$) is difficult to define accurately both from experimental measurements or by calculation. Therefore, the B_0 temperature can only be derived from the B_S temperature.

It has been shown [24] that the temperature difference between the M_0 and M_S temperatures is about 200 °C. Similarly, there is a 50–55 °C temperature difference between the B_0 and B_S temperatures [25].

Since bainite is a non-lamellar mixture of acicular ferrite plates and carbide, the practical upper temperature (B_S) should be determined by the intersection point of the practical equilibrium curves for either

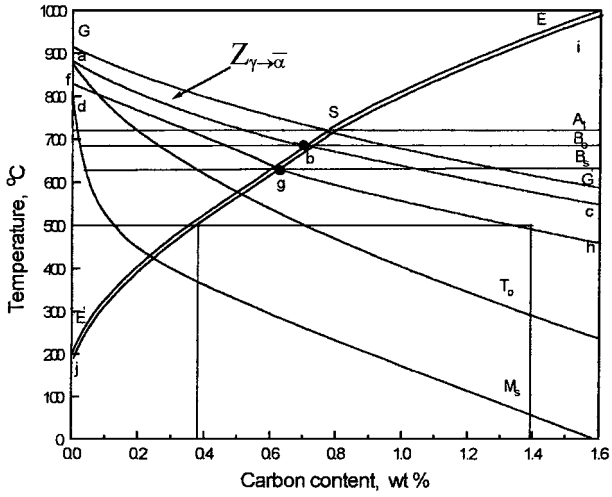

Figure 9 Schematic diagram showing the location of the B_S (*point g*) and B_0 (*point b*) temperatures for plain carbon steels.

ferrite or carbide precipitating from austenite. Radcliffe *et al*. [26], concluded from an analysis of published data that the growth of bainite occurs at a rate that is controlled approximately by the diffusion of carbon in the austenite ahead of the interface. Consequently, they considered that there are no essential differences between Widmanstatten ferrite and bainite in the sense that they are both displacive transformations during which carbon redistributes during growth. Therefore, it is reasonable to use the practical upper temperature limit of Widmanstatten ferrite as the practical upper temperature limit of ferrite in bainite, due to the similar characteristics to the Widmanstatten ferrite, such as coherent precipitation [27], and isothermal formation and retention of the orientation relationships with the parent phase [28]. The upper temperature limit of Mehl [29] (curve *fh*) for the formation of Widmanstatten ferrite and the extrapolated curve† of the upper temperature limit where carbide precipitates from austenite (from Zener [7]) are selected as reference points. The intersection point (point *g*) of the above two curves (curve *fh* and curve *ij*) is the practical upper temperature limit of the bainite reaction (B_S) in FeC alloy steels. This is shown schematically in Fig. 9. It is also evidient from Fig. 9 that the B_S temperature is 630 °C for plain carbon steels. The carbon content at point *g* is about 0.60 wt%–0.65 wt%.

Since the B_0 temperature was already defined as being 50–55 °C higher than the B_S temperature [25], the B_0 temperature should be about 680 °C. Similarly, the B_0 temperature can be determined by the intersection point (point *b*) between the curve $Z_{\gamma\to\vec{\alpha}}$ (curve *ac*) and curve ES (as shown in Fig. 9). The carbon content at point *b* is about 0.75 wt%.

In plain carbon steels, the bainite and pearlite C-curves overlap extensively on account of the pearlite reaction occuring prior to the bainite reaction. The bainite reaction is thus obscured. Therefore, the bainite reaction is only found below 500 °C. As shown in Fig. 9, the carbon content should be between 0.4 wt% and 1.4 wt% at 500 °C for the bainite reaction to proceed. With decreasing temperature, the carbon content at which the bainite reaction will occur will correspondingly increase. This result is similar to Aaronson's findings [5] (as shown in Fig. 10), where the microstructural B_S temperature for 0.4–1.4 wt%C steels remains constant (In his microstructural B_S definition, he restricted the use of the term bainite to structures in which the ferrite component has a plate or needle morphology, which is the approach we have taken.).

The discrepancy between our study and Aaronson's is also easy to explain and understand. As discussed above in this paper, Aaronson [5] considers that the upper limit temperature for bainite formation should be the eutectoidal reaction(A_{e1}). However, this conflicts with a number of experimental results [20, 25] except when the carbon content is lower than 0.4 wt% [5]. At 500 °C, when the carbon content of steel is either lower than 0.4 wt% or higher than 1.4 wt%, the precipitation of proeutectoid ferrite (grain boundary ferrite) or carbides (grain boundary cementite) should occur. This mixed miscrostructure should not be considered the pure "conventional" bainite (a non-lamellar mixture of acicular ferrite plates and carbide [21]) since the allotrimorphic ferrite forms prior to the bainite reaction in some samples. This, of course, give rise to difficulties in the fundanmental interpretation of the experimental data. Also, it turns out that there are certain features of bainite nucleation that can be usefully explored in terms of the driving forces in order to reveal information about rate phenomena. One of these features is the observation that the Widmanstatten ferrite start (W_S) and bainite start (B_S) temperatures are much more sensitive to alloy chemistry than the A_{e3} temperature (the highest temperature at which α-ferrite and austenite can coexist in equilibrium) [30] and the A_{e1} temperature (the highest temperature at which α-ferrite, cementite and pearlite can coexist in equilibrium) [25]. Therefore, from this point, the A_{e1} temperature should not be considered to be identical to the B_S temperature.

4. Effects of chemical composition on B_S temperature

The factors affecting the B_S temperature are mainly those which can change the relative free-energies of austenite, $\vec{\alpha}$-Fe‡ and the carbide [6, 21]. The chemical composition of the steel is the most important of these factors. The carbon content of the steel affects the upper temperature limit at which the $\vec{\alpha}$-Fe and carbide precipitate from the austenite. In the bainite reaction, however, the $\vec{\alpha}$-Fe and the carbide will precipitate from the austenite simultaneously. At that time, the carbon content of steel at the bainite upper temperature limit is constant as is the case for the eutectoid decomposition of pearlite which has a constant carbon content (the eutectoid composition, 0.77 wt%) when its upper temperature limit (about 727 °C) is reached. If not, the

† The solid curve *ES* shows the equilibrium cooling state; the dotted curve *ij* shows the practical cooling state which is about 10–15 °C lower than curve *ES* under normal cooling rates [25].

‡ $\vec{\alpha}$-Fe used in this paper is defined as the ferrite which retains coherency with the parent austenite.

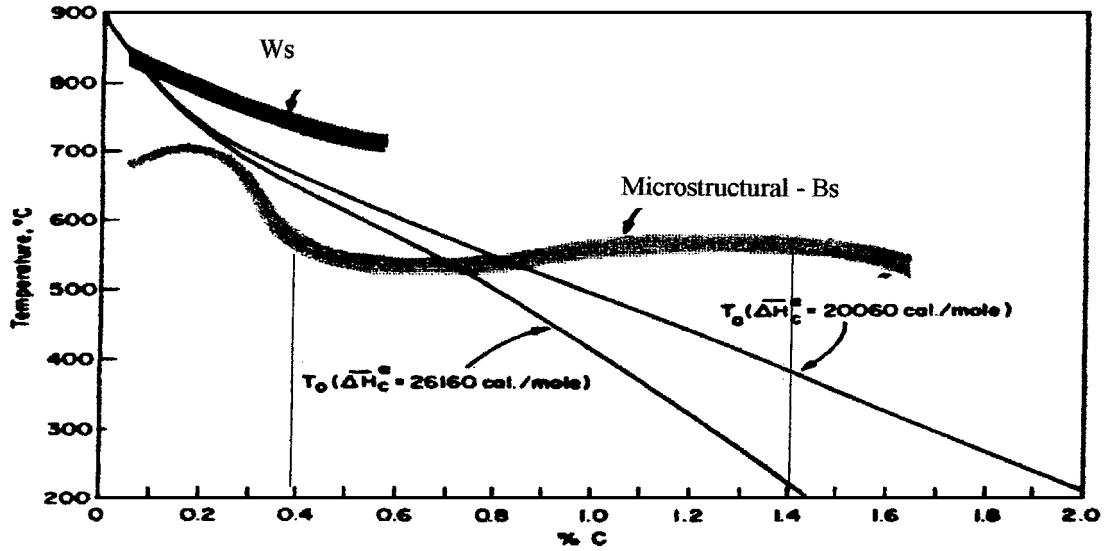

Figure 10 Microstructural-B_S temperature (ferrite is required to be in the Widmanstatten form) and W_S (the Widmanstatten ferrite start) temperature as a function of carbon content in high-purity Fe-C alloys. Also shown are two T_0 vs. %C curves [5].

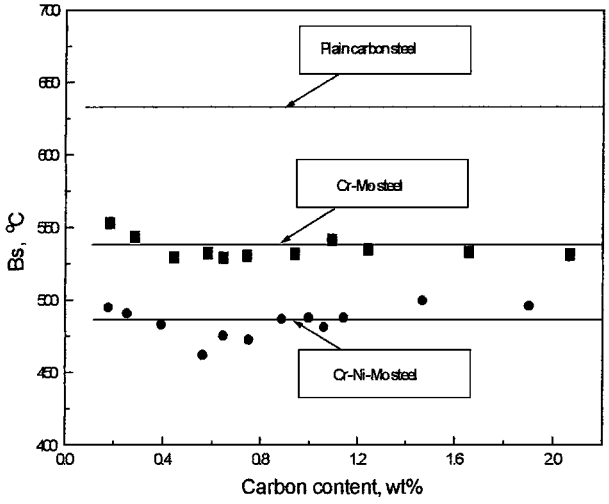

Figure 11 Effects of carbon content on the B_S temperature in Cr-Mo [31] and Cr-Ni-Mo [15] steels.

pro-eutectoid ferrite or cementite precipitates first and causes the composition of the austenite to move towards the eutectoid composition. Therefore, the B_S temperature should be similar to the A_1 temperature, i.e. independent of the carbon content of the steel. In order to verify this hypothesis, we examined the published data on B_S temperature for a Cr-Mo alloy steel [31] and a Cr-Ni-Mo alloy steel [15] which have the same basic alloying elements but different carbon contents. The results are shown in Fig. 11.

The B_S temperature does not change significantly with carbon content. However, the addition of alloying elements other than C to the steel will affect the bainite reaction. These alloying elements change the thermodynamic properties when ferrite precipitates from austenite. However, for the precipitation of cementite, the effect of chemical composition is similar to that for the pearlite transformation [25]. That is the reason why the extrapolated thermodynamic equilibrium curve for the austenite → cementite transformation ($Z_{\gamma\rightarrow C}$) (curve ES) is adopted as the reference curve for the precipitation of carbides in bainite. All common alloying elements reduce B_S in a linear fashion [20, 25, 32], as can be seen in Fig. 12. All these lines intercept the ordinate axis at almost the same point, i.e. 630 °C. The effect of alloying elements on B_S temperature can be described by the slope of the B_S vs. alloy content line.

From the above analysis, together with some new experimental data [32], a new equation is proposed to calculate the practical upper temperature of bainite reaction:

$$B_S(^\circ C) = 630 - 45Mn - 40V - 35Si - 30Cr - 25Mo - 20Ni - 15W \quad (1)$$

This equation can be applied when there is complete austenitization. i.e. the carbide and alloying elements are completely dissolved in the austenite.

5. Test of empirical equations

In order to examine the validity of the three existing empirical equations for B_S due to Zhao [2], Bodnar *et al.* [3] and Steven and Haynes [1] and to compare them with our the new formula, we took experimental B_S temperatures measured from isothermal transformation (IT) diagrams for 82 alloy steels from the "Atlas of Isothermal Transformation and Cooling Transformation Diagrams" [33] and compared them with temperatures calculated using the 4 empirical equations: see Table I. The composition of all 82 steels were within the validity range for Steven and Haynes' equation, namely, carbon: 0.1–0.55%, chromium: trace-3.5%, manganese: 0.2–1.7%, molybdenum: trace-1.0%, nickel: trace-5%. The validity ranges for the empirical equations of Zhao [2] and Bodnar *et al.* [3] are considerably more restricted.

The experimental B_S temperatures could be reliably assessed from the IT diagrams in which there was no appreciable overlap of the bainite and pearlite transformation ranges. Given the effects of different austenitizing conditions, and other differences in the experimental determination of the B_S temperatures, it is reasonable to assume an error of about 25 °C in the subsequent calculations due to these experimental factors. Thus, if

TABLE I Chemical compositions of alloy steels[#] used to test validity of empirical equations [33]

No.	C	Mn	V	Si	Cr	Mo	Ni	W	Page [12]	B_S [1]	B_S [2]	B_S [3]	B_S [4]	B_S [5]
1	0.29	1.64		0.24	0.05	0.45	0.02		52	595	408	563	563	535
2	0.33	1.48		0.18	0.16	0.27	0.26		53	550	388	563	564	540
3	0.38	1.49		0.25		0.41			54	530	378	523	559	544
4	0.39	1.59		0.27	0.16	0.44	0.05		55	515	357	498	532	532
5	0.50	1.50		0.17	0.20	0.45	0.10		58	560	306	434	505	537
6	0.52	1.18		0.30	0.13	0.30	0.16		59	575	325	447	543	552
7	0.38	1.51		0.26	0.99		0.40		60	482	339	438	507	515
8	0.26	1.51		0.42	0.45	0.50			61	604	420	559	551	521
9	0.30	1.63		0.49	0.44	0.33			62	593	398	528	544	518
10	0.19	1.37		0.14	0.20	0.31	0.56		63	580	447	620	595	539
11	0.40	1.34		0.21	0.53	0.22	1.03		64	500	322	463	508	520
12	0.21	0.78			0.99		1.09		96	538	441	575	593	543
13	0.22	0.77			1.99		1.08		97	585	411	492	528	516
14	0.40	0.45			1.52		3.33		102	482	261	405	452	498
15	0.29	0.21		0.056	1.45		3.25		108	477	341	493	511	510
16	0.33	0.57		0.23	0.85	0.09	3.26		109	500	303	430	502	503
17	0.33	0.23		0.06	1.79		3.78		110	448	288	432	455	488
18	0.35	0.44		0.14	1.43	0.13	4.23		111	425	261	428	429	475
19	0.26	0.87				0.26			120	590	491	634	660	584
20	0.39	0.67		0.26		0.49	0.06		123	593	428	568	622	577
21	0.42	0.55		0.25		0.71	0.06		128	593	414	558	606	578
22	0.28	0.65		0.19	0.66	0.22	0.16		144	543	470	582	626	566
23	0.33	0.53			0.90	0.18			152	580	460	543	615	575
24	0.37	0.77			0.98	0.21			153	575	417	498	575	561
25	0.41	0.67		0.23	1.01	0.23	0.20		154	580	391	475	562	552
26	0.42	0.69		0.23	0.94	0.18	0.05		155	593	398	476	572	557
27	0.42	0.72			0.99	0.42	0.05		156	550	364	470	546	556
28	0.46	0.77		0.28	1.06	0.22	0.15		157	566	361	436	538	543
29	0.50	1.25			0.65	0.18			158	538	329	416	522	550
30	0.14	0.26			1.05	0.26	2.21		162	538	456	627	592	536
31	0.17	0.57			0.45	0.24	1.87		163	545	438	642	612	547
32	0.27	0.53		0.26	0.71	0.18	3.38		164	538	330	540	520	504
33	0.30	0.69	<0.01	0.22	0.85	0.30	2.83		165	515	314	553	498	502
34	0.31	0.66		0.28	0.72	0.34	1.67		166	566	362	534	546	527
35	0.31	0.62		0.20	0.64	0.58	2.63		167	490	351	528	500	509
36	0.32	0.61	0.025	0.28	0.63	0.22	3.22	0.16	169	520	306	514	507	501
37	0.32	0.56		0.27	0.74	0.51	2.37		170	522	326	522	511	513
38	0.32	0.47	0.013	0.29	1.21	0.30	4.13	0.11	172	430	269	463	439	470
39	0.33	0.69		0.41	0.72	0.28	1.41		173	510	365	525	553	528
40	0.33	0.51			2.32	0.36	0.82		174	470	368	421	472	512
41	0.35	0.43		0.25	1.55	0.53	2.52		175	400	294	447	451	492
42	0.38	0.69		0.20	0.95	0.26	1.58		176	520	326	474	519	525
43	0.38	0.56		0.15	0.74	0.46	2.42		177	518	297	484	497	517
44	0.39	0.62		0.23	1.11	0.18	1.44		178	520	333	462	523	527
45	0.40	1.38		0.24	0.53	0.16	0.74		179	530	325	465	520	525
46	0.42	0.78			0.80	0.33	1.79		181	538	291	453	497	527
47	0.44	0.58		0.23	1.26	0.11	1.41		182	525	313	424	510	527
48	0.42	0.67		0.31	0.72	0.48	2.53		183	490	265	454	472	505
49	0.51	0.73			0.99	0.45	2.74		184	480	202	372	419	501
50	0.55	0.60			1.03	0.19	0.36		185	565	322	392	526	560
51	0.55	0.83			1.01	0.48	1.15		186	538	247	366	454	527
52	0.39	0.56				0.74	3.53		200	538	262	519	482	516
53	0.33	0.45			1.97				208	538	447	462	563	551
54	0.38	0.20		0.18	2.98				210	500	423	372	501	525
55	0.42	0.68			0.93				211	538	410	478	590	572
56	0.48	0.86		0.25	0.98	0.04	0.18		212	570	352	424	544	549
57	0.43	0.74	0.16		0.92				225	552	401	469	583	563
58	0.53	0.67	0.18		0.93				226	552	360	413	562	565
59	0.23	0.82	0.22		1.22	0.53			227	593	464	560	565	534
60	0.40	0.78	0.22		1.25	0.53			229	538	380	459	520	535
61	0.24	0.69	0.09			0.50	3.35		232	538	343	604	538	516
62	0.24	0.57	0.09			0.48	2.20		233	593	398	630	593	545
63	0.25	0.88	0.23		0.73	0.88	0.59		234	538	410	573	537	526
64	0.25	0.52	0.16	0.15	1.14	0.65	3.33		235	495	313	520	459	478
65	0.27	0.84	0.11		0.73	0.90	0.60		236	538	402	563	534	531
66	0.30	0.80			0.55	0.21	0.54		240	574	427	563	601	561
67	0.44	0.90			0.54	0.22	0.45		242	593	356	475	557	559
68	0.38	1.08		0.70	0.40	0.11	0.34		244	538	387	513	580	535
69	0.14	0.81			0.49	0.27	1.81		256	538	447	642	596	536
70	0.43	1.02			0.48	0.13	0.31		260	538	366	481	566	560
71*	0.22	0.76			0.51	0.20	0.57		261	566	475	616	629	564

(*Continued*)

TABLE I (*Continued*).

No.	C	Mn	V	Si	Cr	Mo	Ni	W	Page [12]	B_S [1]	B_S [2]	B_S [3]	B_S [4]	B_S [5]
72*	0.45	0.89			0.66	0.12	0.59		262	538	344	458	550	555
73*	0.50	0.77			0.50	0.21	0.61		263	552	330	448	551	563
74*	0.46	0.79			0.77	0.18	0.91		266	566	204	445	532	549
75*	0.26	0.55		0.21	3.34	0.54	0.25		272	480	408	390	422	479
76*	0.15	0.92	0.06		0.50	0.46	0.88		275	538	468	643	601	542
77	0.39	0.89	0.03	0.48	0.95	0.50	0.68		277	538	344	470	511	517
78*	0.44	0.79	0.06	1.63	2.10	0.54			278	482	339	368	448	459
79*	0.51	0.72	0.20	0.27	0.94	0.05	0.15	0.11	280	560	352	418	552	546
80	0.49	0.41		0.33	1.87		2.97		290	440	372	332	420	485
81	0.45	0.70	0.20		1.00				311	538	392	453	576	561
82	0.55	0.55						1.96	315	600	388	481	635	577

[#] The amount of element S and P in some steels have not been shown since they have no effect on B_S point.
* Trace amounts of boron present.
B_S^1: B_S temperatures (°C) determined from the actual (experimental) isothermal transformation diagrams,
B_S^2: B_S temperatures (°C) calculated using Zhao's equation,
B_S^3: B_S temperatures (°C) calculated using Bodnar's equation,
B_S^4: B_S temperatures (°C) calculated using the Steven and Haynes' equation,
B_S^5: B_S temperatures (°C) calculated using the present equation.

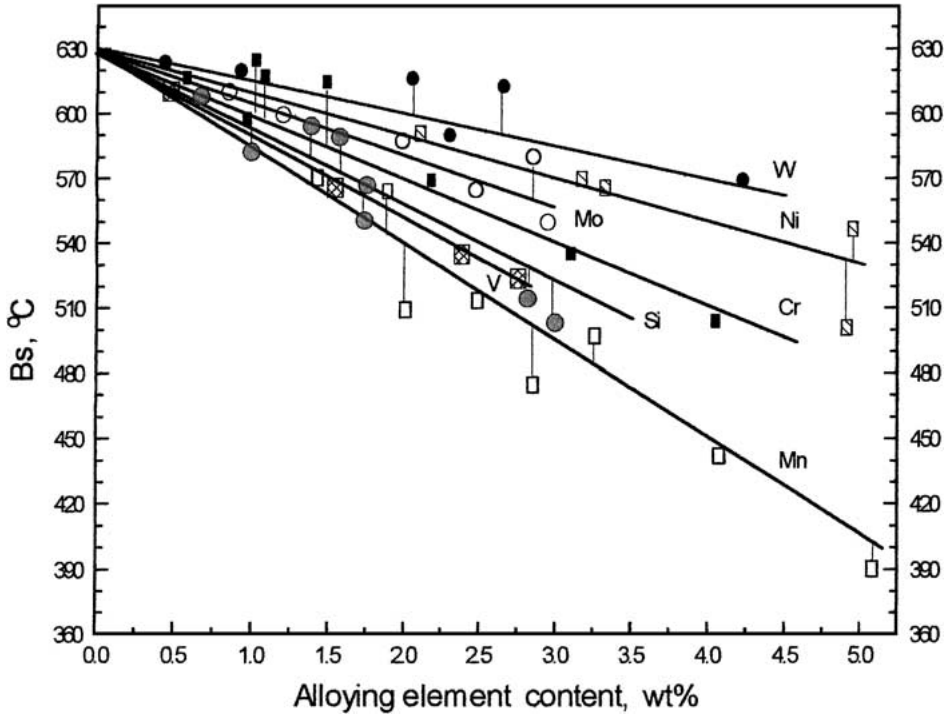

Figure 12 Effect of alloying elements on the B_S temperature [20, 25, 32] in steels.

a calculated B_S temperatures falls within 25 °C of the measured value, it is considered a good fit. The four equations that were compared are as follows:

Zhao's equation [2]:

$$B_S\ (^\circ\mathrm{C}) = 720 - 585.63\mathrm{C} + 126.60\mathrm{C}^2 - 66.34\mathrm{Ni} + 6.06\mathrm{Ni}^2 - 0.232\mathrm{Ni}^3 - 31.66\mathrm{Cr} + 2.17\mathrm{Cr}^2 - 91.68\mathrm{Mn} + 7.82\mathrm{Mn}^2 - 0.3378\mathrm{Mn}^3 - 42.37\mathrm{Mo} + 9.16\mathrm{Co} - 0.1255\mathrm{Co}^2 + 0.000284\mathrm{Co}^3 - 36.02\mathrm{Cu} - 46.15\mathrm{Ru} \quad (2)$$

Bodnar *et al*'s equation [3]:

$$B_S\ (^\circ\mathrm{C}) = 844 - 597\mathrm{C} - 63\mathrm{Mn} - 16\mathrm{Ni} - 78\mathrm{Cr} \quad (3)$$

Steven and Haynes' equation [1]:

$$B_S\ (^\circ\mathrm{C}) = 830 - 270\mathrm{C} - 90\mathrm{Mn} - 37\mathrm{Ni} - 70\mathrm{Cr} - 83\mathrm{Mo} \quad (4)$$

The new equation:

$$B_S\ (^\circ\mathrm{C}) = 630 - 45\mathrm{Mn} - 40\mathrm{V} - 35\mathrm{Si} - 30\mathrm{Cr} - 25\mathrm{Mo} - 20\mathrm{Ni} - 15\mathrm{W} \quad (1)$$

Table II gives a statistical analysis of the data obtained for the B_S temperature using the 4 equations.

TABLE II Summary of statistical analysis of data for B_S temperature obtained using the 4 empirical equations

	Percentage of agreement*	Mean Deviation**	Standard deviation
Zhao's equation	0	51.30	59.90
Bodnar et als equation	18.3	60.26	72.63
Steven and Haynes' equation	46.4	35.61	28.63
The new equation	72.6	30.27	22.61

* The percentage of calculated data that falls within the limit of ±25 °C.
** The mean deviation used in this paper is calculated according to the equation $\frac{\sum|Xi-\bar{X}|}{n}$, which can be used to compare the mean deviation distribution range.

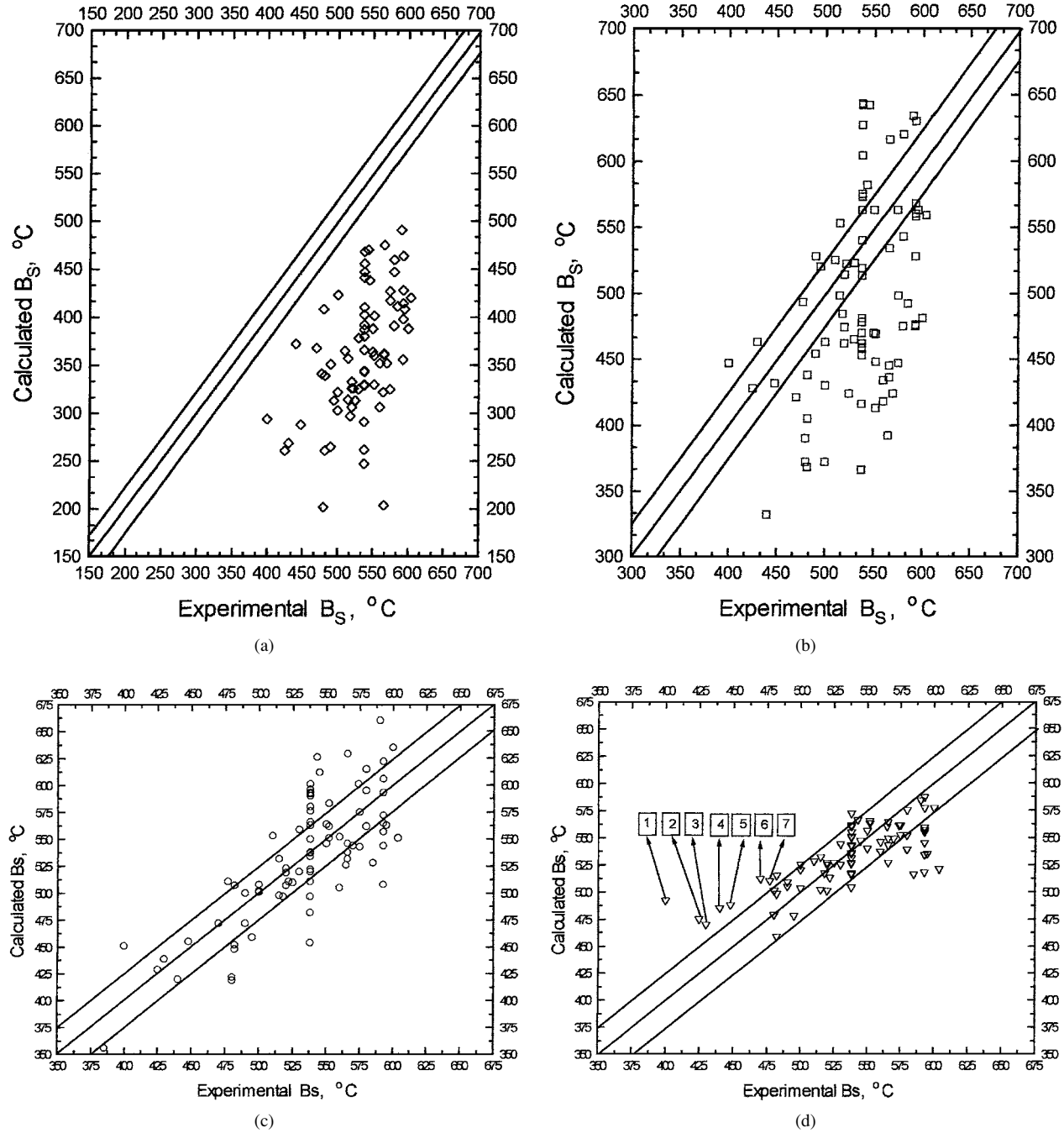

Figure 13 Comparison of experimental B_S values and calculated B_S values for the 82 alloy steels listed in Table I [33] using (a) Zhao's equation [2], (b) Bodnar *et al.*'s equation [3], (c) Steven and Haynes' equation [1] and (d) the present equation. (The 3 solid lines indicate exactly the two deviation limits of ±25 °C from the complete agreement line in the middle.)

The new equation gives a better fit to the experimental results than other three equations when the 82 alloy steels from the handbook [33] were examined. For more than 70 pct of low alloy steels, the B_S temperature can be predicted to within ±25 °C by the new equation. A comparison of the experimental and calculated B_S temperatures are shown in Fig. 13a–d for empirical equations 1–4, respectively. No data point falls within the limits of ±25 °C for Zhao's equation [2] and thus the validity of this equation is questionable. Zhao's considered the B_S temperature to be the transformation start temperature for bainite ferrite, not that for 'conventional' bainite, i.e. ferrite+carbide. Zhao believed that the 'conventional' B_S would be a little higher than the B_S for bainitic ferrite as predicted using his equation. This is borne out in Fig. 13a. Where all data points are distributed below the deviation limit. However, the mean deviation is more than 50 °C.

The large deviations seen when using Zhao's equation might result from insufficient consideration of elemental interaction since his equation was derived from a survey of data for binary alloys (such as, Fe-C, Fe-N, Fe-Ni, Fe-Cr, Fe-Mn, etc.). Zhao did not consider ternary, or higher, alloys at all. Actually, the effects of multicomponent alloying elements are quite complex, and are not merely additive. This was considered in the development of our empirical equation. The agreement between experimental and calculated B_S value using Bodnar *et al.*'s equation is not good. This is not surprising since they only used data from

TABLE III Chemical compositions of data points No. 1–7 [33] in Fig. 13d which show large deviations between measured and calculated B_S values

	1	2	3	4	5	6	7
Cr (wt%)	1.55	1.43	1.21	1.87	1.79	2.32	1.45
Ni (wt%)	2.52	4.23	4.13	2.97	3.78	0.82	3.25
Corresponding Number in Table I	41	18	38	80	17	40	15

22 alloy steels to establish their regression formula. Also, their equation only fits a very narrow composition range (Carbon: 0.15–0.29 wt%, Silicon: 0.01–0.23 wt%, Manganese: 0.02–0.77, Nickel: 0.21–3.61, Chromium: 1.13–2.33, Molybdenum: 0.44–1.37). Even with Steven and Haynes' equation, which has been applied exensively, the percentage agreement is only 46.4%.

Looking for possible 'errors' in our new equation. We see that the discrepancy between measured and calculated B_S temperatures is relatively larger in only two temperature ranges, namely, below 475 °C or over 550 °C. Generally, the calculated B_S temperatures are higher than the experimental B_S in the low temperature range. However, in the high temperature range, the calculated B_S values are slightly lower than the experimental B_S values. Because the deviations for the experimental B_S temperatures below 475 °C, see Fig. 13 d, are for high nickel and chromium alloys (>3% Ni + Cr) (see Table III), the effects of nickel and chromium are possibly underestimated in the new equation. However, the deviations for B_S temperatures over 550 °C can not yet be explained. In spite of this, the new equation has a more extensive applicability in that it agrees with the measured B_S temperatures for more alloy compositions than previous empirical equations.

6. Conclusions

It was Zener's opinion that the B_S temperature is identical to the T_0 temperature. This is not always true when high carbon contents are considered. The model of Fisher for the B_S temperature is invalid since Kriesement and Wever corrected the deviation of Lyman's report, which was used to support Fisher's proposal. Given that the B_S temperature in many steels lies either above 450 °C or below the eutectoid temperature (A_{e1}), the models of either Gyljaev or Aaronson would not appear valid. The model due to Blanter for the B_S temperature can only explain the temperature conditions and characteristics when ferrite is formed, but does not consider the temperature conditions and characteristics for carbide formation. The B_S temperature proposed by Kriesement and Wever is, actually, the B_0 temperature. The lack of agreement between experimental data and calculated data suggests that the model of Kriesement and Wever for B_S requires further refinement. The model of Leont'ev only provids a conceptual view of the upper temperature limit of the bainite reaction, but does not provide any practical temperature data. Thus, all the existing models needed further modification and refinement.

The theoretical upper temperature limit, B_0, for the bainite reaction is determined by the point of intersection between the thermodynamic equilibrium curve for the austenite→ferrite transformation by coherent growth (curve $Z_{\gamma\rightarrow\vec{\alpha}}$) and the extrapolated thermodynamic equilibrium curve for the austenite→cementite transformation (curve *ES* in the Fe-C phase diagram). The theoretical upper temperature limit B_0 for the bainite reaction is about 50–55 °C higher than the practical upper temperature limit, B_S. In plain carbon steels, the practical and theoretical upper temperature limits, B_S and B_0, are about 630 °C and 680 °C, respectively. The bainite reaction is only found below 500 °C in practice because the bainite reaction is obscured by the pearlite reaction which occurs prior to the bainite reaction. At 500 °C, for the bainite reaction to proceed, the carbon content should be between 0.4 wt% and 1.4 wt%. With a further decrease in temperature, the carbon content range over which the bainite reaction occurs is correspondingly increased. The validity of a new empirical equation for the bainite upper temperature limit:

$$B_S\ (^\circ\mathrm{C}) = 630 - 45\mathrm{Mn} - 40\mathrm{V} - 35\mathrm{Si} - 30\mathrm{Cr} - 25\mathrm{Mo} - 20\mathrm{Ni} - 15\mathrm{W}$$

is examined by comparing it with the three other existing empirical equations for the calculation of the B_S temperature of steels. It is shown that the B_S temperature can be predicted to within ±25 °C using this new formula for more than 70 pct of the 82 low alloy steels examined.

Acknowledgments

This study was supported by the Natural Science Research Council of Jilin Province in China. Continued funding is being provided by the Natural Science and Engineering Research Council of Canada through a Research Grant (A4391) awarded to Professor Derek O. Northwood.

References

1. W. STEVEN and A. G. HAYNES, *J. Iron Steel Inst.* **183** (1956) 349.
2. J. ZHAO, *Mater. Sci. and Tech.* **8** (1992) 997.
3. R. L. BODNAR, T. OHHASHI and R. I. JAFFEE, *Met. Trans.* **20A** (1989) 1445.
4. R. F. HEHEMANN, K. R. KINSMAN and H. I. AARONSON, *ibid.* **3** (1972) 1077.
5. H. I. AARONSON, "The Mechanism of Phase Transformations in Crystalline Solids" (The Institute of Metals, London, 1969) p. 270.
6. E. S. DAVENPORT and E. C. BAIN, *Trans. Met. Soc. A.I.M.E.* **90** (1930) 117.
7. C. ZENER, *Trans. Amer. Inst. Min. Met. Eng.* **167** (1946) 550.
8. K. R. KINSMAN and H. I. AARONSON, "Transformation and Hardenability in Steels" (Climax Molybdenum Co., Ann Arbor, MI, 1967) p. 39.
9. A. HULTGREN, *Jerkontorets Ann* **135** (1951) 403.
10. J. R. BLANCHARD, R. M. PARK and A. J. HERZIG, *Trans. Amer. Soc. Metals* **29** (1941) 317.
11. J. C. FISHER, "Thermodynamics in Physical Metallurgy" (Amer. Soc. Metals, Cleveland, OH, 1950) 201.
12. T. LYMAN and A. R. TROIANO, *Trans. Amer. Soc. Metals* **37** (1946) 402.

13. A. P. GYLJAEV, "Thermodynamics Development of Steels" (Mashgis, Moscow, 1960) p. 60 (in Russian).
14. M. E. BLANTER, "Phase Transformation on the Thermodynamics Development of Steels" (Metallurgisdat, Moscow, 1962) p. 129 (in Russian).
15. O. KRIESEMENT and F. WEVER, in Symposium on the Mechanisms of Phase Transformation in Metals, Monograph and Rep. Ser. no 18 (Applied Science Publishers Ltd., London, 1955) p. 253.
16. S. A. LEONT'EV, *Physics of Metals and Metallurgy* **16** (1963) 516 (in Russian).
17. H. KRAINER, M. KRONEIS and R. GATTERINGER, *Archivfür das Eiserhüten Wesen* **26** (1955) 131 (in German).
18. H. I. AARONSON, H. A. DOMAIN and G. M. ANDES, *Trans. Met. Soc. A.I.A.E.* **236** (1960) 753.
19. H. I. AARONSON, *Trans. Met. Soc. A.I.M.E.* **212** (1958) 212.
20. Z. ZHAO, C. LIU, D. O. NORTHWOOD and D. WANG, *Rare Metal Materials and Engineering* **28**(4) (1999) 206 (in Chinese).
21. J. M. ROBERTSON, *J. Iron Steel Inst.* **119** (1929) 391.
22. E. S. DAVENPORT and E. C. BAIN, *Trans. Met. Soc. A.I.M.E.* **90** (1930) 117.
23. Z. ZHAO, D. O. NORTHWOOD, C. LIU, Y. LIU and D. WANG, in The Third Pacific Rim International Conference on Advanced Materials and Processing (PRICM3), edited by M. A. Imam *et al*. (The Mineral, Metals & Materials Society, 1998) p. 193.
24. M. COHEN, E. S. MACHLIN and V. G. PARANJPE, "Thermodynamics in Physical Metallurgy" (Amer. Soc. Metals, New York, 1949).
25. YUNXU LIU, "Principles of Heat Treatment" (Mechanical Industry Press, Beijing, 1981) p. 76 (in Chinese).
26. S. V. RADCLIFFE, M. SCHATZ and S. A. KULIN, *J. Iron Steel Inst.* **201** (1963) 143.
27. T. KO and J. ZHAO, *Acta Metallurgica Sinica* **1** (1956) 201 (in Chinese).
28. R. F. MEHL, C. S. BARRETT and D. W. SMITH, *Trans. Met. Soc. A.I.M.E.* **105** (1933) 218.
29. R. F. MEHL and A. DUBE, "Phase Transformation in Solids" Wiley, (New York, 1955) p. 99.
30. A. ALI and H. K. D. H. BHADESHIA, *Mater. Sci. and Tech.* **6** (1990) p. 781.
31. H. KRAINER, M. KRONEIS and R. GATTERINGER, *Archivfür das Eiserhüten Wesen* **26** (1955) 131 (in German).
32. CHENG LIU, Ph. D. dissertation, Harbin Institute of Technology, Harbin, China, 1998 (in Chinese).
33. H. E. BOYER, "Atlas of Isothermal Transformation and Cooling Transformation Diagrams" (Amer. Soc. Met., Metals Park, OH, 1977) p. 52.

Received 30 March 1999
and accepted 21 March 2001